2021

Optimization of Refrigerant Compositions for Low-GWP Refrigerant Mixtures Using Segment-by-segment Heat Exchanger and Detailed System Models

Zhenning Li
Oak Ridge National Laboratory, United States of America, liz5@ornl.gov

Bo Shen

Kyle Gluesenkamp

Optimization of Refrigerant Compositions for Low-GWP Refrigerant Mixtures Using Segment-by-segment Heat Exchanger and Detailed System Models

Zhenning Li[1], Bo Shen[2]*, Kyle Gluesenkamp[3]

[1,2,3]Oak Ridge National Laboratory, Oak Ridge, TN, 37830 USA
[1]Tel: 301-503-8568, [2]Tel: 865-574-5745, [3]Tel: 865-241-2952
Email: [1]liz5@ornl.gov, [2]shenb@ornl.gov, [3]gluesenkampk@ornl.gov

* Corresponding Author

ABSTRACT

The recently introduced hydrofluoroolefin (HFO) refrigerants, including R1234yf and R1234ze(E), have significantly lower global warming potentials (GWPs) than traditional hydrofluorocarbon (HFC) refrigerants like R410A. However, prior tests show that direct drop-in of pure R1234yf or R1234ze(E) into equipment designed for R410A results in a decrease in heat exchanger capacity and the system coefficient of performance. The primary reason is the lower in-tube heat transfer performance of R1234yf and R1234ze(E) compared with that of R410A. To address this issue, previous studies have mixed the mildly flammable HFC R32 with HFOs to improve system performance, with HFC R125 also added to suppress flammability. Previous studies selected compositions based on simple cycle analyses and did not consider modifications of the heat exchanger circuitry configuration to adapt to the new refrigerants. This study presents a novel multi-objective optimization approach to design a refrigerant composition that maximizes energy efficiency within flammability and GWP limits. The approach in this work simultaneously optimizes mixture composition and heat exchanger circuitry configuration. A case study on a rooftop unit indicates that, compared with mixture-only optimization, simultaneous optimization of mixture and heat exchanger circuitry yields a 5.9% improvement in cycle efficiency and a 48.6% reduction in refrigerant flammability with a GWP of 268. Circuitry optimization using refrigerants with different temperature glides shows that the larger the temperature glide is, the larger EER improvement is obtained. The results show that zeotropic blends with a large temperature glide are more sensitive to the refrigerant circuitry than pure refrigerants and may suffer significant performance degradation with subpar heat exchanger circuitry design. The proposed optimization approach is generally applicable to mixtures with any number of components. Using this approach to design a HVAC system can yield higher system efficiency within flammability and GWP constraints.

1. INTRODUCTION

Modern cooling technologies are significant sources of greenhouse gas emissions (GHGs) with total CO_2 equivalent emissions from the HVAC sector accounting for 7.8% of global GHG emissions (Coulomb et al., 2017). Considering the commitment to reduce the impact of GHGs on climate in HVAC&R sector, a transition from fluorinated substances to alternative refrigerants with reduced global warming potential (GWP) values is supported by F-gas Regulation (Schulz and Kourkoulas, 2014), the Montreal Protocol with the Kigali Amendment (Clark and Wagner, 2016), and the Paris Agreement (2015). The requirements as set forth by the F-gas Regulation banned the use of refrigerants with a GWP of 2500 or greater for high refrigerant charge stationary HVAC equipment in 2020. Beginning in 2022, a GWP limit of 150 has been set for multi-circuit cascade systems for commercial use with a nominal capacity of 40 kW or more, and for 2025, the GWP limit for single split AC on the European Union (EU) market is set as 750. This ban will not permit the use of R410A (2088 as GWP value) in small charge system applications. In this regard, much research has been conducted to find the alternative low-GWP refrigerants.

McLinden et al. (2017) identified 138 low-GWP refrigerants by screening more than 60 million chemical formulas. They filtered out the refrigerants according to several criteria. For instance, only molecules that consist of eight chemical elements were chosen, and the maximum number of atoms in a molecule was limited to 18. In addition, the critical temperature was limited to between 320K and 420 K. After filtering out highly toxic and unstable fluids, the screening identified 23 fluids with GWP values below 1000. ANSI/ASHRAE Standard 34 (2016) added six new pure substances and 40 new mixtures by considering the trade-off between GWP and flammability. While the majority of the new nonflammable refrigerant mixtures have been formulated as alternatives for R134a and R404A, only one new nonflammable mixture, R463A, was proposed as an alternative to R410A. Therefore, there is strong interest in developing more low- or non-flammable alternatives to R410A with a GWP lower than R410A.

Typical criteria for new refrigerant mixture development include factors such as increasing volumetric cooling capacity, improving energy efficiency, reducing GWP, and reducing flammability. To develop low-GWP refrigerants, hydrofluoroolefins (HFOs) are commonly used as components in the mixture. For R410A alternatives, Bobbo et al. (2018) reviewed the experiment data of 16 HFO refrigerants and their mixtures. They concluded that only R1234yf and R1234ze(E) have been extensively investigated in terms of the thermodynamic and transport properties. Therefore, R1234yf with a GWP of 4 is one of the best component candidates to replace R410A. However, R1234yf has much a smaller latent heat than R410A; thus, the coefficient of performance (COP) of a heat pump system would be decreased if R1234yf were used alone. To maintain the system performance, Domanski et al. (2017) proposed that refrigerant mixtures of R1234yf and other fluids with large latent heat be used, such as R32, since R32 can contribute to increased system performance and heat exchanger (HX) cooling capacity due to its high volumetric cooling capacity and large latent heat. To form the R410A alternative mixtures, R125 is one of the commonly supplied HFCs in HVAC industry and is widely used to suppress the flammability. Table 1 lists the characteristics of R32, R1234yf, R125, R410A, and several R410A alternative mixtures in terms of the ozone depletion potential (ODP), GWP, temperature glide and ASHRAE safety class (2016), and mixture compositions. The temperature glides are evaluated at saturation pressure corresponding to 8 °C dew-point temperature.

Table 1: Comparison of characteristics of selected refrigerants

Refrigerant	ODP	GWP	Temperature Glide [K]	ASHRAE Safety Class	Compositions
R32	0	675	0	A2L	-
R1234yf	0	4	0	A2L	-
R125	0	3500	0	A1	-
R410A	0	2088	0.1	A1	50.0% R32 / 50% R125
R452A	0	1127	3.8	A1	11.0% R32/59.0% R1234yf /30.0% R125
R452B	0	1363	1.1	A2L	67.0% R32/7.0% R1234yf /26.0% R125
R452C	0	1014	3.4	A1	12.5% R32/61.0% R1234yf /26.5% R125
R454A	0	2140	5.5	A2L	35.0% R32/65.0% R1234yf
R454B	0	698	1.3	A2L	68.9% R32/31.1% R1234yf
R454C	0	2220	7.6	A2L	21.5% R32/78.5% R1234yf

To achieve a low GWP, low flammability, and high system performance, the compositions of the R32/R1234yf/R125 mixture should be carefully determined. Fujitaka et al. (2010) experimentally compared the COP of a room air-conditioner with a R32/R1234yf mixture with that of R410A and concluded that the COP increased with an increase in R32 composition in the mixture but was slightly lower than the COP using R410A. Okazaki et al. (2010) tested R32/R1234yf mixture in a room air-conditioner and concluded that the mixture having 60% R32 yields more than 93% of the annual performance factor of R410A. Trade-offs among system performance, flammability, and GWP were observed in these studies. Abdelaziz et al. (2016) conducted experiments to compare R410A and its alternatives in small residential mini-split applications and large commercial packaged rooftop units (RTUs). All previous studies focused on drop-in replacements of refrigerants without modifications of the equipment.

Shen et al. (2018) found that if retrofits with minor equipment modifications of the existing systems are implemented, the detrimental variations in system performance due to the drop-in alternative refrigerants can be mitigated. Shen et al. (2018) enumerated different circuitry patterns of the tube-fin condenser and tube-fin evaporators used in a R410A RTU and simulated the RTU performance using different R410A alternatives. They found that redesigning HX circuitry configurations can make the new refrigerant more compatible to the system. In the literature (Li et al., 2019),

HX circuitry optimization has proven to be a convenient and cost-effective way to improve the system performance because it only modifies the tube connections (i.e., hairpins) without changing other structural parameters for a HX.

A literature review of previous research led to the conclusion that when developing low-GWP mixtures, trade-offs between different refrigeration selection criteria need to be considered and no fully design-compatible mixture has been identified for various applications as an all-in-one solution. With this goal in mind, designing a new mixture for specific applications to satisfy multiple criteria can be formulated as a multi-objective optimization problem. This paper aims at presenting a novel low-GWP alternative refrigerant mixture optimization framework that can make the new mixture more compatible with the systems by redesigning the HX circuitries. The remainder of the paper is organized as follows. Section 2 details the new optimization approach. Section 3 demonstrates the efficacy of the proposed approach through case studies. Section 4 provides the conclusions of this study.

2. METHODOLOGY

2.1 System Simulation Model

The DOE/ORNL Heat Pump Design Model (HPDM) (Shen and Rice, 2016) is used to model the performance of an air-conditioning system. The HPDM is a public-domain HVAC equipment and system modeling and design tool which supports a free web interface and a desktop version for public use. Some features of the HPDM related to this study are introduced below.

Compressor model: To compare refrigerant performances, it was assumed that the compressor has the same volumetric efficiency (η_{vol}=95% in Equation (1)) and isentropic efficiency ($\eta_{isentropic}$=70% in Equation (2)).

$$m_r = Volume_{displacement} \times Speed_{rotation} \times Density_{suction} \times \eta_{vol}, \quad (1)$$

$$Power = m_r \times (h_{\text{discharge,s}} - h_{\text{suction}}) / \eta_{isentropic}, \quad (2)$$

where m_r is compressor mass flow rate; *Power* is compressor power; η_{vol} is compressor volumetric efficiency; $\eta_{isentropic}$ is compressor isentropic efficiency; h_{suction} is compressor suction enthalpy; $h_{\text{discharge,s}}$ is the enthalpy obtained at the compressor discharge pressure and the suction entropy; and $Speed_{rotation}$ is the motor rotational speed.

Heat exchanger model: A finite volume (segment-to-segment) tube-fin HX model is used to simulate the performance of the HX with different circuitries. This model has been validated by the experiment data from Abdelaziz et al. (2016). The dehumidification model used in the evaporator simulation is from Braun et al. (1989). Details can be seen in Shen et al. (2018).

Expansion device: Isenthalpic process is assumed in the expansion process.

Fans: The airflow rate and power consumption are direct inputs from the laboratory measurements for the model calibrations.

Refrigerant Lines: Temperature changes and pressure drops in suction, discharge, and liquid lines are specified using the measured data from the experiments.

Refrigerant Properties: REFPROP version 10.0 (Lemmon et al., 2018) is used to simulate the new refrigerant mixtures by making the mixture definition file according to the required format.

For more details on the HPDM, see Shen and Rice (2016).

2.2 Optimization Algorithm

In this research, the Particle Swarm Optimization (PSO) algorithm (Kennedy and Eberhart, 1995) implemented in GenOpt (Wetter, 2001) is integrated with HPDM. GenOpt provides an interface to integrate with simulation tools, and HPDM provides the numerical function evaluation, which is computationally expensive and for which derivatives are not available. Particle Swarm Optimization is extensively used in various problem domains due to its broad applicability, ease of use and global search feature. PSO is a population-based stochastic optimization algorithm. It mimics the social behavior of members of bird flocks or fish schools to determine the location of each particle in the next generation. Each design is a particle, and the set of designs in each iteration step is a population. PSO begins by creating the initial particles and assigning them initial velocities. It evaluates the objective function at each particle location and determines the best (lowest) fitness value as well as the best location in one population in order to choose new velocities to move the particles. It iteratively updates the particle velocities and locations until the convergence criterion is reached.

Because the optimization algorithms in GenOpt only support single objective optimization, this study extends the capability of GenOpt to conduct multi-objective optimization by implementing the weighted sum method. For

instance, the two objectives of this research are maximizing the system energy efficiency ratio (EER) while minimizing refrigerant flammability (detailed in Section 2.4). Equation (3) shows how the fitness value of a design is calculated by the weighted sum method. The w_1 and w_2 are weights set by the user of this framework. The relative values of the weights reflect the different priorities of different objectives. The optimal designs are achieved through minimizing the fitness value. When conducting optimization under different weights, a Pareto front can be obtained (Arora, 2004).

$$fitness = w_1 \times EER^{norm} + w_2 \times Flammability^{norm},\ where\ w_1 + w_2 = 1 \tag{3}$$

Because the weighted sum method depends on comparing the values of different objectives, those values usually have different units and/or different orders of magnitude. It is necessary to normalize the objectives. Equation (4) and Equation (5) show the normalized EER and normalized flammability, respectively. The minus sign in front of *EER(x)* in Equation (4) transforms the maximization problem to a minimization problem. In Equation (4), EER_{max} and EER_o are constants to represent the upper limit and the lower limit EERs in the design space, respectively. Similarly in Equation (5), $Flammability_{max}$ and $Flammability_o$ are the upper and lower limits of the flammability values in the design space, respectively. Obviously, those upper and lower limits cannot be known before running the optimization; however, the approximated values of those limits are sufficient to maintain the objectives in the same order of magnitude (Arora, 2004). In this study, those upper and lower limits are obtained by a few hundreds of preliminary HPDM simulations.

$$EER^{norm} = \frac{EER_{\max} - EER(x)}{EER_{\max} - EER_o}. \tag{4}$$

$$Flammability^{norm} = \frac{Flammability(x) - Flammability_o}{Flammability_{\max} - Flammability_o}. \tag{5}$$

2.3 Case Study

In this paper, HPDM has been closely calibrated against experiment data from drop-in alternative performance evaluations conducted by Abdelaziz et al. (2016) on the commercial packaged R410A RTU. The RTU is a 39.9 kW (11 ton) R-410A system; its power supply is 460V, 3 Phase, 60 Hz. It uses a single-speed scroll compressor. The condenser fan moves 10200 CFM (4.81 m^3/s) across the outdoor HX and consumes 1720 W of power; the indoor blower provides 3715 CFM (1.75 m^3/s) of supply airflow and consumes 1235 W of power. Table 2 lists the empirical correlations used for local heat transfer and pressure drop calculations during the performance evaluation of the condenser and evaporator of the RTU. As the refrigerants used in this study are zeotropic mixtures, the proper selection of the flow condensation and flow boiling correlations are crucial to have accurate prediction of the heat transfer coefficients for zeotropic mixtures. Heat transfer during boiling of mixtures involves sensible heating of mixture and mass transfer resistance. To take these two effects into consideration, the correction factor proposed in Thome and Shakir (1987) is used with the boiling correlation from Wojtan et al. (2005). Similarly, the condensation of mixtures involves sensible cooling of mixture and mass transfer resistance. To predict condensation heat transfer coefficient, Thome et al. (2003a) correlation is used with correction proposed by Bell and Ghaly (1972). Bell and Ghaly (1972) found that mass transfer is roughly proportional to heat transfer and heat transfer is much easier to calculate than mass transfer. Their method assumes the equilibrium between the different phases. They neglect the mass transfer resistance and compensate the neglection of mass transfer resistance by overestimating the sensible heat transfer resistance.

Table 2: Correlations adopted in condenser and evaporator simulations

Operating Mode	Heat Transfer Correlations	Pressure Drop Correlations
Refrigerant - Liquid Phase	Dittus and Boelter (1985)	Blasius (1907)
Refrigerant - Two Phase Boiling (Evaporator)	Wojtan et al. (2005) with correction factor from Thome and Shakir (1987)	Choi et al. (1999)
Refrigerant - Two Phase Condensation (Condenser)	Thome et al. (2003a) with correction factor from Bell and Ghaly (1972)	Choi et al. (1999)
Refrigerant - Vapor Phase	Dittus and Boelter (1985)	Blasius (1907)
Air	Wang et al. (1999)	Wang et al. (1999)

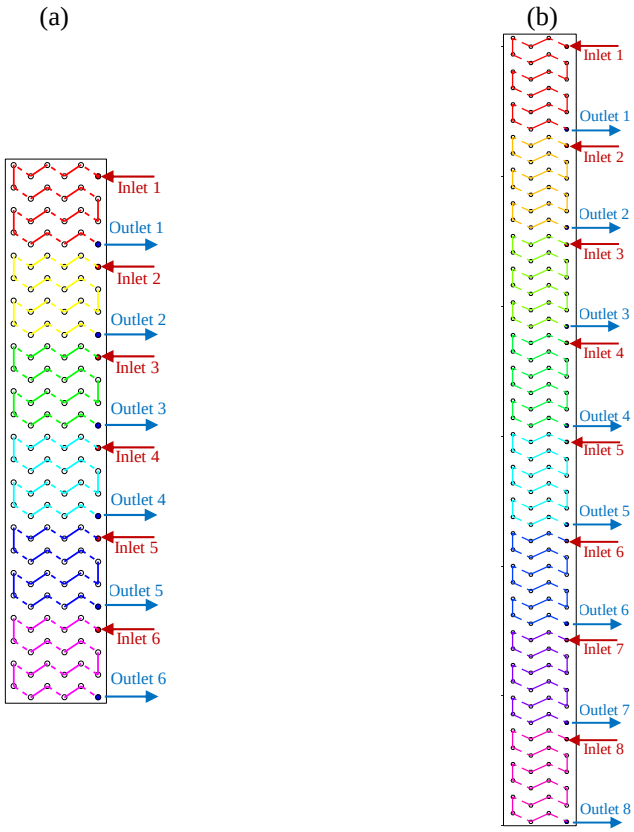

Figure 1: Baseline circuitry of heat exchangers in packaged rooftop unit (a) evaporator and (b) condenser.

The circuitries of the baseline R410A evaporator and condenser are shown in Figure 1(a) and Figure 1(b), respectively. The evaporator has 144 tubes and 6 banks and is divided into 6 mixed flow circuits. The condenser has 192 tubes and 4 banks and is divided into 8 mixed flow circuits. In Figure 1, a solid line represents a U-bend (i.e., hairpin) on the front end of the HX, while a dotted line represents a U-bend on the farther end. The different colors represent different circuits. The distributor distributes the refrigerant into the inlet tube of each circuit.

2.4 Problem Formulation

Considering the demands to improve system performance and guarantee safety, the problem is formulated as a bi-objective optimization problem. To quantify the refrigerant flammability in the system, two factors need to be taken into consideration. The first factor is the flammability of the mixtures, which depends on their molecular structure. The second factor is the system refrigerant charge, since one common approach to guarantee safety is to reduce system charge when using flammable refrigerants. Thus, Equation (6) defines the flammability of the refrigerants in the RTU.

$$Flammability = \Pi \times \text{System Charge}, \tag{6}$$

where Π is the flammability index of the mixture, which is predicted using the empirical model developed by Linteris et al. (2019). This model uses this flammable index to assess the flammability of refrigerants based on their molecular structures. Table 3 lists the flammability indexes of R32, R1234yf, and R125. The negative flammability index of R125 indicates its utility as a flammability suppressor.

Table 3: Flammable index of selected refrigerants predicted by Linteris et al. (2019)

Refrigerants	Flammable Index (Π)
R32	35.6
R1234yf	6.9
R125	-34.7

Equation (7) shows the problem formulation. The objectives are to maximize the system EER of the RTU and to minimize the refrigerant flammability. A set of continuous design variables is the mass fraction (or "composition") of each of the *n* components. Each design variable is constrained between 0 and 1, and the sum of all compositions is constrained to be 1. In previous research, Shen et al. (2012) developed an optimization framework that integrates HPDM with GenOpt to perform automatic calibration of a heat pump model based on experiment data. This study extends the capability of the previously developed optimization framework by adding circuitry configuration as the discrete design variables. Specifically, the discrete circuitry configuration variable varies among three patterns, counterflow, mixed flow, and parallel flow, as illustrated by a six-tube HX in Figure 2.

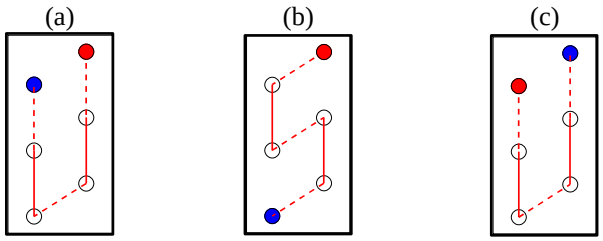

Figure 2: Heat exchanger circuitry patterns: (a) counterflow, (b) mixed flow, (c) parallel flow.

The circuitry optimization conducted in this paper is different from those conducted in Li et al. (2019) where the length of different circuit can be different, and different circuits in one HX can interleave with each other. In this paper, the optimal circuitries are constrained to have regular patterns. That is, each circuit has the same number of tubes, and the U-bends (hairpins) are constrained to connect the adjacent tubes only. This guarantees the resulting circuitry to be cost-effective with short production lead time. Because the evaporator has 24 tubes in each bank, the number of circuits is a discrete variable which varies among all common divisors of 24. Similarly, the condenser has 48 tubes in each bank, so the number of circuits is a discrete variable varying among all common divisors of 48. To simulate the performance of the RTU, the cooling capacity of the evaporator and the evaporator outlet superheat degree are fixed to be the same as those of the original R410A RTU; the compressor displacement volume is automatically altered to meet the target evaporator cooling capacity. The condenser outlet subcooling degree is adjusted along with the mixture compositions and HX circuitry configurations to achieve the optimum EER. In Equation (7), the last constraint limits the GWP value of the mixture. The GWP of R410A is set as the upper limit for new mixtures with the goal of developing R410A alternatives with a lower GWP. The GWP value of the mixture is estimated based on the linear weighted sum of the actual GWP of known substances (Schulz and Kourkoulas, 2014).

$$
\begin{aligned}
&Objective\text{-}1:\ Maximize(EER)\\
&Objective\text{-}2:\ Minimize(Flammability)\\
&Subject\ to:\\
&\quad 0\% \le Composition_1 \le 100\%\ ,\ 0\% < Composition_k < 1 - \sum_{i=1}^{k-1} Composition\\
&\quad \sum_{i=1}^{n} Composition_i = 1\\
&\quad \text{HX Circuit Pattern} \in \{\text{counter flow, mixed flow, parallel flow}\}\\
&\quad N_{circuits,\,evaporator} \in \{1,2,3,4,6,8,12,24\}\\
&\quad N_{circuits,\,condenser} \in \{1,2,3,4,6,8,12,16,24,48\}\\
&\quad \Delta T_{superheat,evaporator,outlet} = 6.7\ K\\
&\quad 5.6\ K \le \Delta T_{subcooling,condenser,outlet} \le 8.3\ K\\
&\quad Q_{evaporator} = 39.92\ kW\\
&\quad GWP_{\text{mixture}} \le 2088\ (GWP_{\text{R410A}})
\end{aligned}
\tag{7}
$$

3. RESULTS

3.1 Results for Binary Components Mixture Optimization

To illustrate the benefits of simultaneous optimization of mixture composition and HX circuitry, two optimization runs are conducted. The first run optimizes the mixture compositions alone, and the HXs circuitry configurations are fixed as the baseline circuitries in Figure 1. The second run optimizes the mixture compositions and HX circuitry configurations simultaneously. For all the optimization runs presented in this paper, the population size of PSO is 40 and the number of generations is 40. The multi-objective optimizations are performed by varying the weight of EER from 0% to 100% with 10% as the interval to generate the Pareto fronts.

Figure 3 shows the Pareto fronts for the two optimization runs for binary (R32/R1234yf) mixtures in terms of system EER and refrigerant flammability. The EER and flammability are normalized based on the values of the baseline R410A RTU. The size of the marker shows the scale of the GWP value. A number of trade-offs among flammability, EER, and GWP are clearly shown in Figure 3. A large fraction of R32 provides such benefits as increasing EER but also has disadvantages such as increasing the flammability index (Π) and increasing GWP. Large fractions of R1234yf reduce the flammability and GWP but are detrimental to EER due to R1234yf's inferior thermo-hydraulic properties.

Figure 3 includes two Pareto fronts: one for mixture-alone optimization and one for mixture and HX simultaneous optimization. The distance between the two Pareto fronts demonstrates that simultaneously optimizing the mixture compositions and HX configurations yields significant performance improvements compared with optimizing the mixture compositions alone. Figure 3 also shows the performance for the reference refrigerants (R452A, R452B, R452C, and R410A) in the baseline system. The Pareto front to optimize the mixture and HXs simultaneously, as shown in blue circles, dominates all the other solutions in terms of increasing EER and reducing flammability, while it consists of inferior designs dominated by a baseline system with R410A.

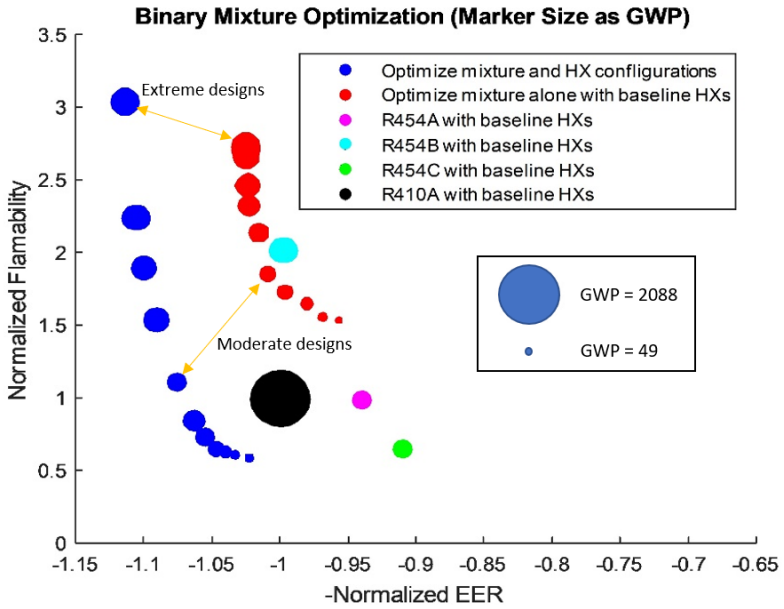

Figure 3: R32/R1234yf mixtures optimization results compared with off-the-shelf refrigerants**.**

In the Pareto fronts, the extreme optimal designs of which the EER weight is 100% and the moderate optimal designs of which the EER weight is 50% are highlighted. For the extreme optimal designs, circuitry optimization increases the normalized EER by 8.7% from 1.03 to 1.12. For the moderate optimal designs, circuitry optimization increases the EER by 5.9% from 1.02 to 1.08 while reducing the normalized flammability by 48.6% from 2.14 to 1.11. The GWP of the moderate design with circuitry optimization is 268, which is significantly less than that of R410A.

3.2 Results for Ternary Components Mixture Optimization

Similar to the previous section, two sets of optimization runs are conducted for ternary (R32/R1234yf/R125) mixture optimization. Figure 4 shows the Pareto fronts for the two optimization runs with and without including HX circuitry configurations as design variables. The marker sizes of most points in Figure 4 are significantly larger than those in Figure 3, which is attributed to the addition of R125 (3500 as GWP) in the mixture. It can be seen that the positions of both Pareto fronts in Figure 4 are lower than the positions of the Pareto fronts in Figure 3 because R125 significantly reduces the flammability.

It is worthwhile to mention that the higher GWP value of the ternary mixtures is also attributed to the specific problem formulation (i.e., maximizing EER and minimizing flammability) used in this paper. Because GWP is only considered to be a constraint rather than an optimization objective, R1234yf is not the most desirable component because its performance on EER and flammability is neutral. The optimizer depends on adding R32 to improve EER and R125 to reduce flammability. If minimizing GWP is an optimization objective, different results can be expected. The purpose of the case study is to demonstrate the efficacy of the proposed optimization approach, rather than promoting the specific results under a specific problem formulation. According to the application scenario, the problem can be formulated differently to satisfy the needs of the decision maker.

In Figure 4, the performances of the optimal designs obtained from the optimizing mixture and HX configurations simultaneously dominate the off-the-shelf mixtures (R452A, R452B, R452C) as well as the optimal designs from optimizing with the mixture alone. These results once again demonstrate the efficacy to optimize mixture compositions and HX configurations simultaneously.

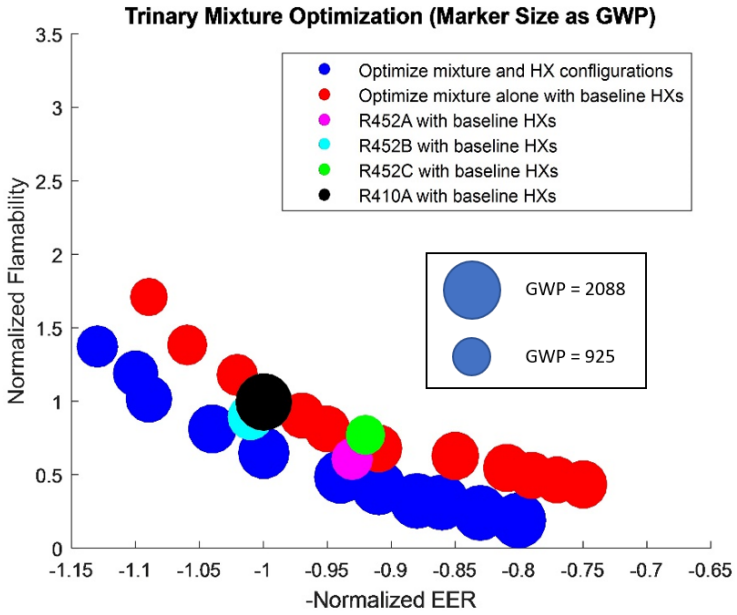

Figure 4: R32/R1234yf/R125 optimization results compared with off-the-shelf refrigerants.

3.3 Effect of Mixture Compositions on System Performance

For zeotropic mixtures, it is worthwhile to investigate the effect of mixture temperature glide on performance improvements obtained from heat exchanger circuitry optimization. To achieve this goal, a separate circuitry optimization practice is conducted using the off-the-shelf refrigerants listed in Table 1. The problem formulation is the same as that shown in Equation (7) except the reduction of design variables. Since the off-the-shelf refrigerants are used in the heat exchangers, the mixture compositions are not the design variables anymore. With these practices, we are aiming to assess the potential of HX circuitry optimization for refrigerants with different temperature glides. Figure 5 shows the EER improvement from heat exchanger optimization for different refrigerant compared with baseline system. The optimal systems shown in Figure 5 are corresponding to design obtained using 100% EER weight, i.e. the optimization runs are single objective optimizations with the only objective to improve EER.

Figure 5 demonstrates that R1234yf has the lowest EER improvement (4.4%) from circuitry optimization and R454C has the highest EER improvement (6.2%). From Table 1, R454C has the highest temperature glide among all refrigerants. Comparing the EER improvements among these refrigerants, the larger the temperature glide is, the larger EER improvement is obtained from circuitry optimization. The results show that zeotropic blends with a large temperature glide are more sensitive to the refrigerant circuitry than pure refrigerants and may suffer significant performance degradation with subpar heat exchanger circuitry design. These results emphasize the necessity for optimizing refrigerant circuitries for zeotropic mixtures.

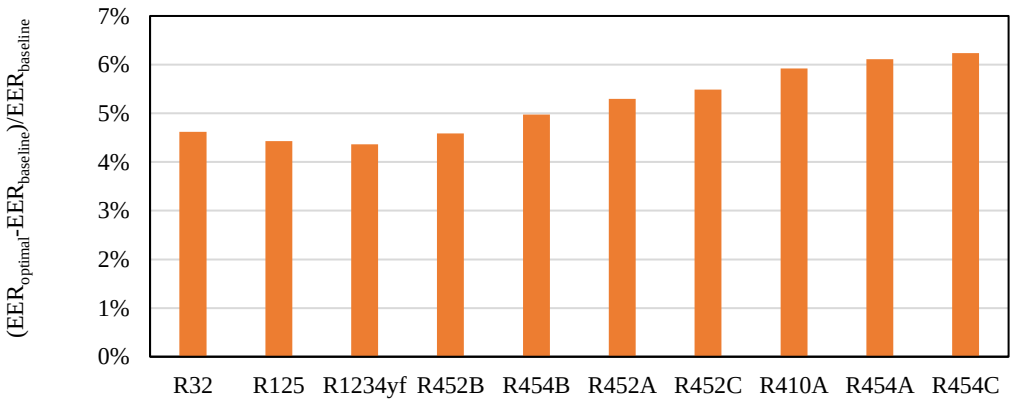

Figure 5: EER Improvements from heat exchanger circuitry optimization for off-the-shelf refrigerants compared with the baseline system

4. CONCLUSIONS

A novel low-GWP refrigerant mixture composition optimization framework is presented in this paper. To improve the new refrigerants' compatibility to the system, the condenser and evaporator circuitry configurations are optimized simultaneously with the mixture compositions. The case studies using an experimental validated R410A RTU show that the proposed optimization approach can generate new binary and ternary mixtures and new circuitry designs to improve system EER, reduce refrigerant flammability, and maintain a low GWP. A case study on a RTU indicates that, compared to mixture-only optimization, simultaneous optimization of mixture and HX circuitry yields a 5.9% improvement in cycle efficiency and a 48.6% reduction in flammability with a GWP of 268. Circuitry optimization using refrigerants with different temperature glides shows that the larger the temperature glide is, the larger EER improvement obtained. The results show that zeotropic blends with a large temperature glide are more sensitive to the refrigerant circuitry than pure refrigerants and may suffer significant performance degradation with subpar heat exchanger circuitry design. The proposed optimization approach is generally applicable to mixtures with any number of components. Using this approach to design a HVAC system can yield a higher system efficiency within flammability and GWP constraints.

5. ACKNOWLEDGEMENT

The authors would like to acknowledge the funding and support that we receive from the US Department of Energy Building Technologies Office and Mr. Antonio Bouza, the Emerging Technologies lead on heating, ventilating, air-conditioning, water heating, and appliance research.

6. REFERENCES

ANSI/ASHRAE Standard 34–2016, Designation and Safety Classification of Refrigerants" (2016).

Abdelaziz, O., S. Shrestha, B. Shen, A. Elatar, R. Linkous, W. Goetzler, M. Guernsey. and Y. Bargach (2016). Alternative Refrigerant Evaluation for High-Ambient-Temperature Environments: R-22 and R-410A Alternatives for Rooftop Air Conditioners, ORNL/TM-2016/513, Energy and Transportation Science Division, Oak Ridge National Laboratory, Oak Ridge, TN.

Agreement, P. (2015). Paris agreement. Report of the Conference of the Parties to the United Nations Framework Convention on Climate Change (21st Session, 2015: Paris). Retrived December, HeinOnline.

Arora, J. S. (2004). Introduction to Optimum Design, Elsevier.

Bell K.J. and Ghaly M.A. (1972). “An approximate generalized design method for multicomponent/partial condensers.” In AIChE Symp. Ser. (Vol. 69, pp. 72-79).

Blasius, H. (1907). Grenzschichten in Flüssigkeiten mit kleiner Reibung, Druck von BG Teubner.

Bobbo, S., G. Di Nicola, C. Zilio, J. S. Brown and L. Fedele (2018). "Low GWP halocarbon refrigerants: A review of thermophysical properties." International Journal of Refrigeration 90: 181–201.

Braun, J. E., S. A. Klein, and J. W. Mitchell (1989). "Effectiveness models for cooling towers and cooling coils." ASHRAE Trans. 95 (Pt 2).

Choi, J.Y., Kedzierski, M.A. and Domanski, P.A. (2001). “Generalized pressure drop correlation for evaporation and condensation in smooth and micro-fin tubes.” Proceedings of IIF-IIR Commission B1, pp.9-16.

Clark, E. and S. Wagner (2016). "The Kigali Amendment to the Montreal Protocol: HFC Phase-Down." Ozon Action UN Environment (UNEP): 1–7.

Coulomb, D., J. Dupont and V. Morlet (2017). "The impact of the refrigeration sector on the climate change. 35th Informatory Note on Refrigeration Technologies." Paris (France).

Dittus, F. and L. Boelter (1985). "Heat transfer in automobile radiators of the tubular type." International Communications in Heat and Mass Transfer 12(1): 3–22.

Domanski, P. A., R. Brignoli, J. S. Brown, A. F. Kazakov and M. O. McLinden (2017). "Low-GWP refrigerants for medium and high-pressure applications." International Journal of Refrigeration 84: 198–209.

Fujitaka, A., T. Shimizu, S. Sato, and Y. Kawabe (2010). "Application of low global warming potential refrigerants for room air conditioner." 2010 International Symposium on Next-generation Air Conditioning and Refrigeration Technology, Tokyo, Japan.

Kennedy, J. E. and R. Eberhart (1995).“Particle Swarm Optimization.” Neural Networks, The IEEE International Conference on Neural Networks.

Lemmon, E. W., Bell, I. H., Huber, M. L., & McLinden, M. O. (2018). "NIST Standard Reference Database 23, NIST Reference Fluid Thermodynamic and Transport Properties Database (REFPROP): Version 10.0." Gaithersburg, MD.

Li, Z., Aute, V., & Ling, J. (2019). “Tube-fin heat exchanger circuitry optimization using integer permutation based genetic algorithm.” International Journal of Refrigeration, 103, 135-144.

Linteris, G. T., I. H. Bell, and M. O. McLinden (2019). "An empirical model for refrigerant flammability based on molecular structure and thermodynamics." International Journal of Refrigeration 104: 144–150.

McLinden, M. O., J. S. Brown, R. Brignoli, A. F. Kazakov, and P. A. Domanski (2017). "Limited options for low-global-warming-potential refrigerants." Nature Communications 8(1): 1–9.

Okazaki, T., H. Maeyama, M. Saito, and T. Yamamoto (2010). Performance and reliability evaluation of a room air conditioner with low GWP refrigerant. 2010 International Symposium on Next-Generation Air Conditioning and Refrigeration Technology, Tokyo, Japan.

Schulz, M. and D. Kourkoulas (2014). "Regulation (EU) No 517/2014 of The European Parliament and of the council of 16 April 2014 on fluorinated greenhouse gases and repealing Regulation (EC) No 842/2006." Off. J. Eur. Union 2014(517): L150.

Shen, B., O. Abdelaziz, and K. Rice (2012). "Auto-calibration and control strategy determination for a variable-speed heat pump water heater using optimization." HVAC&R Research 18(5): 904–914.

Shen, B., O. Abdelaziz, S. Shrestha, and A. Elatar (2018). "Model-based optimizations of packaged rooftop air conditioners using low global warming potential refrigerants." International Journal of Refrigeration 87: 106–117.

Shen, B. and K. Rice (2016). "DOE/ORNL heat pump design model." Web link: http://hpdmflex. ornl. gov.

Thome, J. R., J. El Hajal, and A. Cavallini (2003a). "Condensation in horizontal tubes, part 2: new heat transfer model based on flow regimes." International Journal of Heat and Mass Transfer 46(18): 3365–3387.

Thome, J. R., & Shakir, S. (1987). “A new correlation for nucleate pool boiling of aqueous mixtures.” In Heat Transfer: Pittsburgh 1987.

Wang, C.-C., C.-J. Lee, C.-T. Chang, and S.-P. Lin (1999). "Heat transfer and friction correlation for compact louvered fin-and-tube heat exchangers." International Journal of Heat and Mass Transfer 42(11): 1945–1956.

Wetter, M. (2001). GenOpt-A generic optimization program. Seventh International IBPSA Conference, Rio de Janeiro.

Wojtan, L., Ursenbacher, T., & Thome, J. R. (2005). „Investigation of flow boiling in horizontal tubes: Part II—Development of a new heat transfer model for stratified-wavy, dryout and mist flow regimes.” International Journal of Heat and Mass Transfer, 48(14), 2970-2985.